InkJet Printing for Mailing Applications

Judith Auslander, Donald Mackay, and Claude Zeller
Pitney Bowes, Shelton, Connecticut, USA

John C. Briggs and Ming-Kai Tse
QEA, Inc., Burlington, Massachusetts, USA

Abstract

In inkjet printing for mailing, the diverse range of available envelope papers poses significant challenges for reliable readability of printed barcodes. If not properly controlled, ink/media interactions, in particular ink sorption, can result in unacceptable degradation in print quality, directly affecting machine readability. Several commercially available aqueous inkjet inks and several recycled and regular envelopes were tested by conventional methods and by ultrasonic attenuation. In this case study, we printed a selected set of envelope papers at low speed (office inkjet printing) with carefully designed test patterns and performed a statistical analysis to correlate print quality attributes and machine readability. Print quality attributes were measured according to ISO-13660 definitions, which are well suited for automated measurement. To elucidate the correlation between paper characteristics and print quality attributes, sorption measurements were also obtained on the same set of envelope papers. Machine readability data were obtained from a verifier reading AIM print quality parameters from DataMatrix symbols. The results of the case study not only provide insight into the correlation between print quality attributes and machine readability but also demonstrate the practical value of implementing ISO-13660 in barcode print quality.

Introduction

Automation of mail sorting by the world's postal services requires machine-readable addresses and postal codes. Automatic postage payment verification programs, such as the USPS Information Based Indicia Program (IBIP)[1] and the Royal Mail's Integrated Mail Processor (IMP) extend this requirement to the indicium. To automate mail processing, postal services worldwide are introducing technical specifications for digital franking machines and new electronic postage standards. The UPU[2] and USPS[1] require printing a two-dimensional barcode in the Postal Revenue Block with a successful readability rate of 99.5% to 99.8%. To achieve these high readability rates, certain print quality attributes must be within acceptable limits.

The barcode industry has little experience using 2D barcodes in a non-controlled (open system) environment such as mailing. **No international standards exist** for print quality attributes of machine-readable postal indicia (or franking marks).

The objective of this paper was to understand the effect of ink/media interaction on print quality attributes measured by an automated print quality measurement instrument IAS-1000 (QEA) as well as by a verifier (Metanetics) that measures print quality growth as well as readability. The correlation between the two measurement systems was evaluated as well as the influence of specific ink/media characteristics on critical print quality attributes such as print growth, raggedness, and blurriness. The samples used for analysis were 2D barcodes (DataMatrix) printed with three printers on four selected envelope types at five module sizes (module size is the physical size of a printed bar). The module size was varied to determine a limit for machine readability for each printer/envelope combination. The resolution and drop volume varied from printer to printer, but for simplification, we measured the print quality attributes as a final output without testing the other variables. Resolution and drop volume dependence will be the subject of another paper.

Ink/media interactions are among the most significant factors affecting print quality, which in turn affect machine readability of barcodes or characters. Inkjet printing using aqueous-based inks is the preferred printing method in home offices and small businesses.[11] Thus, aqueous-based inks will be the only type of inks investigated in this study.

To develop some understanding of the most important issues affecting print quality, many physical and chemical characteristics of the inks and envelopes were measured. The envelopes were characterized for parameters such as pore size, critical surface energy, roughness, sizing, and pH.[3,4,5] The inks were characterized for surface tension, viscosity, and pH, which are all critical ink properties.

The sorption characteristics of the ink/envelope combinations were also determined. The contact angle of a drop of ink placed on the envelope surface was measured as a function of time. This contact angle depends on many factors including penetration, porosity, pore size, and surface energy. Spreading is enhanced[6] by rough surfaces for liquids with contact angles less than ninety degrees and is inhibited by rough surfaces for contact angles greater than ninety degrees.

Additional study of ink wetting, spreading, and penetration was performed using the Bristow wheel apparatus. Many successful studies[7,8,11] have used Bristow dynamic wetting measurements to predict drying time and print quality. Measurements from an ultrasonic attenuation technique[12] were used to complement the data from the Bristow wheel tests. The two methods measure the wetting delay found with rough papers and water-based inks and the penetration rate. A third method, Hercules sizing time, measures the effect of internal sizing on ink penetration.

Ink/Media Measurements

Envelopes

In this study, we focused on four envelope types (A, B, I, and L), which represent extreme characteristics ranging from alkaline recycled to rosin-sized regular and recycled envelopes. The envelopes were tested for roughness, air flow porosity, pore size distribution, pH and critical surface energy. Critical surface energy was determined from Zisman and Owens/Wendt theories. The results are shown in Table 1 and Table 2. Envelopes B and L, which have the highest absorption rate, show the highest Owens/Wendt polar component of the critical surface energy.

Table 1**. Surface Roughness Measurements on Envelopes**

Env	Description	Parker Print Surf(μm)	Sheffield Smoothness (ml/min in^2)	Pore volume at 10μl
A	24#white wove	5.42	152	.226
B	24# white wove	6.23	145	.252
I	recycled	7.68	195	.240
L	recycled, copier grade	7.12	195	.297

Table 2**. Zisman and Owens/Wendt Critical Surface Energy**

Env.	PH & Internal Sizing	Zisman Surface energy (mN/m)	Owens/Wendt (mN/m)	
			Dispersive	Polar
A	4.9 (rosin)	35.40	39.55	0.87
B	8.4 (alkaline)	28.28	28.75	2.28
I	4.1 (rosin)	38.87	44.17	0.41
L	8.4 (alkaline)	37.81	33.69	6.24

Mercury porosimetry was used to determine the pore size distribution of the different envelope types. The measurements were performed on a Micromeritics Autopore III. All the envelopes have a similar pore distributions and median pore diameter (4-5μ). Envelopes I and L show a bimodal distribution of pore sizes. The volume of large pores is a measure of surface roughness. This volume is compared with the data obtained from Parker Print Surf and Sheffield Smoothness in Table 1.

Inks

The surface tension, viscosity, pH, and contact angle of the three inks used in this study[3] were determined and the results are shown in Tables 3 and 4. The same inks were used for envelope absorption tests and in the barcode printing tests. As expected, the contact angle decreases from ink C with the highest surface tension to ink H with the lowest. Ink H absorbs very fast on all envelopes.

Table 3**. Ink Properties**

Printer	Ink	Viscosity (cp)	Surface tension (de Nouy) (dyne/ cm)	Surface Tension (Wilhelm) (dyne/cm)	pH
1	C	2.00	54.9	52.44	8.5
2	F	1.00	42.9	41.9	8.3
3	H	2.9	32.6	30.17	7.8

Table 4**. Contact Angle Measured by Kruss Contact Analyzer**

Env.	Ink C		Ink F		Ink H	
	t=0	t=1 min	t=0	t=1min	t=0	t=1min
A	81.5	66.4	56.0	0 (30s)	30.4	0 (5 s)
B	82.7	74.1	73.4	65.4	36.3	0 (5 s)
I	107.0	105.6	87.7	82.9	24.1	0 (10 s)
L	54.4	0 (40s)	50.0	0 (5s)	10.5	0 (5 s)

Table 5**. Acoustic Wetting Measurements**

Env	Ink C		Ink F		Ink H	
	t_w (ms)	Slope 1/s	t_w (ms)	Slope 1/s	t_w (ms)	Slope 1/s
A	1026	0.43	181	1.51	66.0	38.9
B	846	0.78	133	1.60	34.0	42.8
I	828	0.26	541	0.62	14.0	75.8
L	170	9.99	63.5	29.9	33.0	74.7

The ink-media absorption was tested by Bristow wheel, by Hercules sizing test, and by ultrasonic attenuation. The ultrasonic attenuation data is shown in Table 5. The other data was presented in reference 0.

Ultrasonic attenuation[12] measures the attenuation of an ultrasound beam across an interface of liquid/paper over a predetermined time. The ultrasonic attenuation of the various envelopes in contact with the inks was measured by the Ultrasonic Wetability Tester (UWT-3). Measurements correlate to the amount of sizing in the paper and to Bristow and Hercules measurements.

Bristow measurements were performed with the Paprican Dynamic Sorption Tester BA 92. The contact times varied from 20 to 2000 msec.

Print Quality Measurements

Generating Print Samples

Samples using DataMatrix symbology and various module sizes were printed with three commercial printers.

The elements of interest are described below.

Testing DataMatrix

Tests were applied to DataMatrix 2D barcodes printed with three office printers on a selected set of four envelopes. These printers used the inks described previously. The symbols were created using module sizes ranging from 254µm to 508µm (0.010 to 0.020 inches). A designed experiment was created with each combination of printer, module size, and envelope type. This represented a total of 60 different combinations (3 printers x 4 envelope types x 5 module sizes = 60). For each combination, 20 sample envelopes were printed for increased statistical confidence. These specimens were used to obtain readability measurements made using a barcode verifier. All symbols were created according to the ANSI/AIM specification.[14]

Table 6**. ISO-13660 Print Quality Attributes**

Character and Line		Large Area	
1	Blurriness	1	Darkness, large area
2	Raggedness	2	Background Haze
3	Line width	3	Graininess
4	Darkness, character	4	Mottle
5	Contrast	5	Extraneous marks, background
6	Fill	6	Voids
7	Extraneous marks, character field		
8	Background haze, character field		

Print Quality Tests

The print quality tests described in this paper have been carried out on a high-resolution Image Analysis System (IAS) designed to automate the collection of print quality data from sample images. The QEA IAS-1000 is currently being used to measure the print quality of inkjet printing devices being considered for use in Pitney Bowes mailing and addressing products. Data collection and analysis are carried out in compliance with the methods and procedures described in the International Standard ISO 13660. Table 6 lists print quality attributes defined in the standard. To ensure readability, images should be required to meet certain minimum print quality specifications. The ISO attributes are a logical first choice for consideration in developing these specifications.

To expedite testing, we printed multiple patterns on the test envelopes. These patterns consist of 2D barcodes and a series of lines of various widths. The printed materials, exclusive of the 2D barcodes, are used for print quality analysis.

Verification

Verification is an essential component of any automatic identification application, ensuring quality symbol generation and, as a result, down-line scannability. In this study we used a commercial verifier that is a complete DataMatrix symbol verification system that provides both 100% compliance with AIM Uniform Symbology Specification for DataMatrix symbology and verification reliability.[14] The instrument identifies overall symbol grade, reference decode, symbol contrast, print growth, axial non-uniformity, and unused error correction (UEC), which is used as a measure of readability. The UEC parameter tests the extent to which regional or spot damage in the symbol has eroded the reading safety margin that error correction provides. The amount of UEC is calculated as follows

$$UEC = 1 - \left(\frac{(e + 2t)}{E_{cap}} \right) \quad (1)$$

where e = the number of erasures, t = the number of errors, and E_{cap} = the error correction capacity of the symbol. If no error correction has been applied to the symbol and if the symbol decodes, the value of UEC is taken as 100%.

This portable matrix code verifier provides a large field-of-view and it is designed for symbols up to 38mm (1.5") by 28mm (1.1"), making it ideal for supporting 2D symbologies. The model features self-calibration and output of reporting via an RS-232 interface. A value-added feature is the device's ability to capture and retain the image of the verified symbol for further analysis.

Correlation of Print Quality with Readability

The statistics of the principal print quality attributes and symbol quality parameters have been compiled for all samples tested. We analyzed the print quality attributes of inkjet printing on envelope paper and reduced the parameters that control the print quality for machine readability to the most significant—blurriness and print growth.

Print growth tests that the graphical features comprising the symbol have not grown from nominal so much that they hinder readability with less optimal imaging conditions than the test condition. The print growth parameter—the extent to which dark or light markings appropriately fill their module boundaries—is an important indication of process quality that affects reading performance.

Analysis of the results permits quantification of the effects of ink-media interactions and substrate dependence on readability.

Table 7 shows the summary of print quality results obtained for the four envelopes and three printers with the IAS-1000 (QEA) and Verifier (Metanetics).

Upon examining the print growth data from the verifier and the IAS-1000, we found there was generally a good correlation, as shown in Figure 1. However, there was some amount of scatter in the data, as well as an offset of about 17µm. The most probable explanation of these differences relates to differences in measurement methodology. The IAS-1000 employs ISO-13660 procedures for measuring line width that are slightly different from the methods employed by the verifier. The most likely difference is in the thresholding scheme. In addition, there are also significant differences in lighting and magnification (IAS-1000 uses much higher magnification than the verifier). This illustrates the importance of applying international

standards so that measurements from different devices are more comparable.

Table 7. **Print quality Attributes for Different Printers and Envelopes**

PRINTER	ENVELOPE	Blurriness (µm)	Raggedness (µm)	Print Growth (µm) Vert. Orientation QEA	Vert. Orientation Verifier	Horz.Orientation QEA	Horz.Orientation Verifier
1	A	198.95	13.73	70.11	48.14	60.77	44.58
	B	189.03	12.18	66.59	49.33	76.38	46.88
	I	180.35	12.14	46.88	27.78	47.07	19.16
	L	192.79	16.75	80.60	67.61	88.34	64.83
2	A	184.50	15.74	80.27	66.55	62.70	55.55
	B	163.02	16.83	74.08	61.83	62.35	61.39
	I	160.85	14.13	36.56	8.65	21.86	7.20
	L	199.65	19.80	82.75	68.31	65.24	69.06
3	A	174.65	18.42	82.19	47.62	61.82	49.25
	B	85.93	15.64	95.20	64.76	80.39	58.65
	I	106.99	22.44	141.22	101.63	133.26	95.29
	L	91.39	16.26	93.72	70.32	73.20	63.96

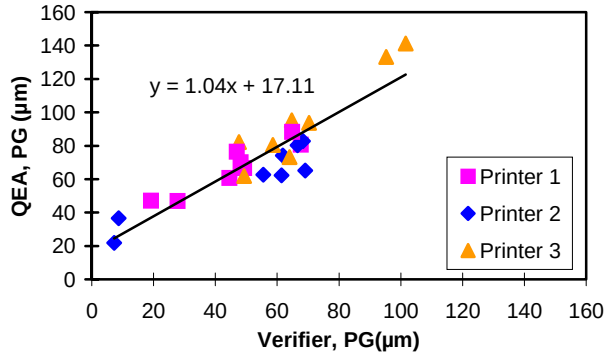

Figure 1. *Correlation of Print Growth on Two Measurement Systems*

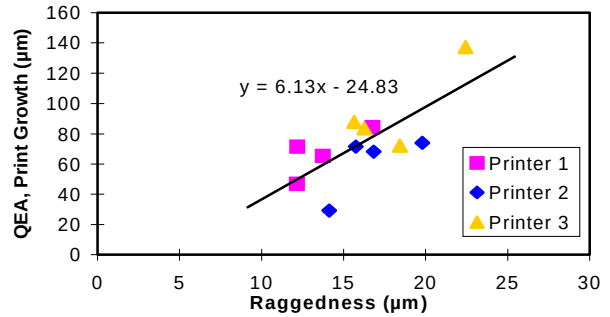

Figure 2*. Relationship between Print Growth and Raggedness*

Also when we try to correlate print growth with raggedness, we get a reasonably good correlation, showing that these attributes are closely related, as shown in Figure 2. In inkjet printing, the same physical mechanism (ink bleeding or wicking) tends to increase print growth and raggedness together. Other printing technologies may have different behaviors.

We plotted the UEC data versus the ratio of print growth to module size for each paper/printer combination, as shown in Figures 3 to 5.

From the data it can be seen that over some range of print-growth-to-module-size ratio, UEC is at 100%, indicating that no Error Correction was required in decoding the symbol. The UEC begins to decrease very dramatically at some threshold value of the print-growth-to-module-size ratio. This indicates a rapid degradation in symbol quality and readability. These threshold values are the most important parts of the curves. With enough statistical evaluation, we should be able to determine the print quality level required to achieve any given read rate (e.g., 99.5%).

This threshold value of print growth varies with ink and paper, from 8% to about 20%, compared to 25% for print growth artificially created on high-quality laser printers or other printing systems previously investigated.[4] The cause of the variability is investigated in this paper.

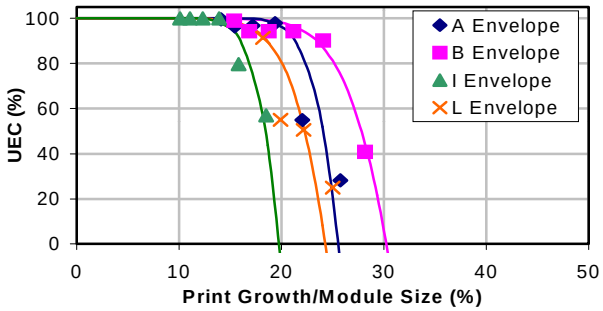

Figure 3*. Print Growth vs. Percentage UEC for Printer 1*

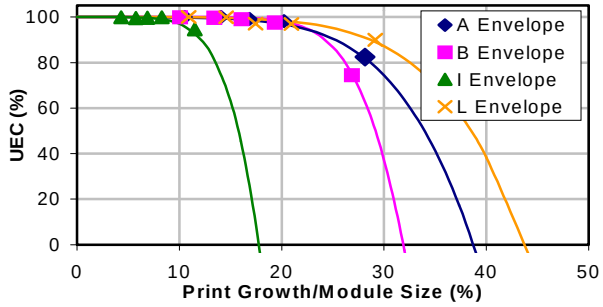

Figure 4*. Print Growth vs. Percentage UEC for Printer 2*

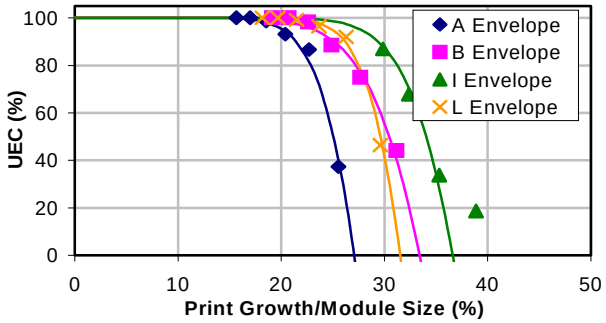

Figure 5. *Print Growth vs. Percentage UEC for Printer 3*

Analysis of the experimental results permits a quantification of the effects of ink/media interactions and printing system dependence on readability with the help of the following formula:

$$UEC_{(pg)} = 1 - \frac{TB_{40}}{E_{40}} \cdot \left[1 - erf\left[\frac{\sqrt{2}}{2} \cdot \frac{(PG_{crit} - pg)}{SIG} \right] \right] \qquad (2)$$

Equation 2 describes the phenomenological/statistical relation between UEC and print gain (pg). Print gain is the ratio of print growth (PG) to the nominal module size. TB_{40} is the total number of codewords (data + error capacity) and E_{40} is the error capacity of the ECC 200 DataMatrix symbol of size 40x40 used in this study. PG_{crit} = 0.5 is a critical tolerance limit whose value has been carefully determined by an independent study on print growth artificially created on high-quality laser printers. The parameter SIG, which is a measure of the readability of the symbol, has been calculated for the entire set of experimental data as a solution of Equation 2 for each data point (module size/printer/paper).

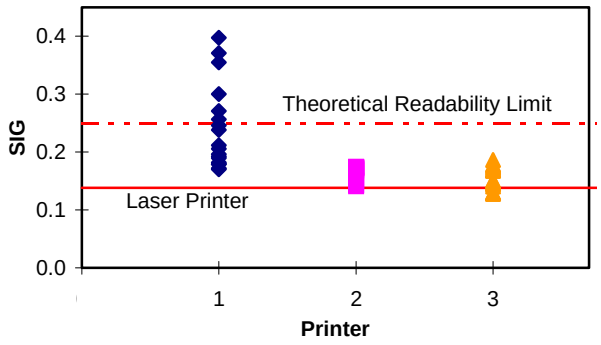

Figure 6. Relationship between SIG and printer type.

Figure 6 shows the range of values of the parameter SIG for the three printers used in this study. The lower line in the graph is set at SIG = 0.138, value found in the laser printer study,[16] and fits precisely the minimum value of each of the three printers. The upper line, set at 0.25, corresponds to UEC 50% (Grade B) and D'50% (Grade A) according to AIM Specification. D' is the AIM print growth parameter equal to 1/0.3 the relative print growth.

Inspection of Figure 6 shows that the range of permissible SIG values for good readability is largely exceeded by printer 1. A careful study of the experimental data suggests that the large values of SIG are caused by a compounding effect of print gain and blurriness. Blurriness is the measurement of the distance over which the transition from the outer boundary (the light or 10% boundary) and the inner boundary (dark or 90% boundary) of the line occurs as defined by ISO 13660.[13] Depending on the printing technology, many factors can contribute to increased blurriness, including media type, toner blast, and coating type. In this case, the increase in blurriness is probably due to the presence of satellite ink drops near the line edge.

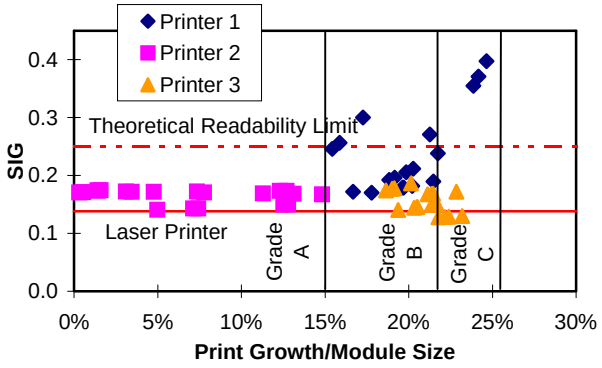

Figure 7. Relationship between SIG and print growth.

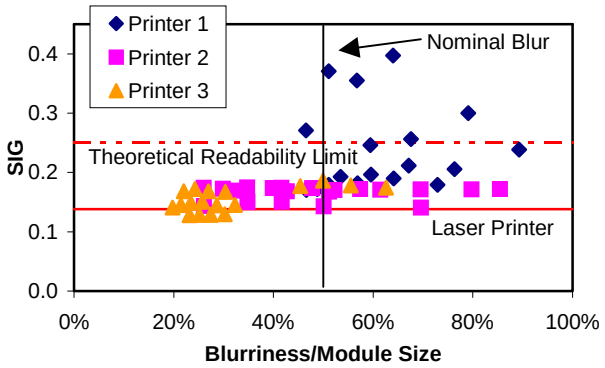

***Figure 8**. Relationship between SIG and blurriness.*

Figures 7 and 8 show plots of SIG vs. print gain and SIG vs. blurriness/module-size, respectively. Conditions of decreased readability (UEC 50%) are obtained when simultaneously the print gain exceeds 15% (Grade B) and the blurriness-to-module-size ratio exceeds 50%.

We believe that this compounding effect affects the modulation of the symbol. Factors such as print growth, the optical characteristics of the substrate, and uneven printing (i.e., blurriness) may reduce the apparent margin between the reflectance of a module and the global threshold. Modulation, if excessive, may reduce the probability of a module being correctly identified as dark or light. In ISO/IEC WD 15415, which is under development, modulation is one of the print quality attributes along with print growth, symbol contrast, and axial non-uniformity.

If we had chosen to display this read rate data in separate plots as measured with the verifier, we would have found that these particular plots (not shown in this paper) are not very insightful in that there are data points with low print growth that use a large amount of EC and values with high print growth requiring little EC. In addition, the data points distribution is erratic. The UECs do not display the same uniform decrease as was seen for each of the same ink/paper combinations when plotted against the print growth measured by the ISO 13660 method.

Correlation between Print Quality and Readability

In this paper we have shown that print growth and blurriness are important print quality attributes that, when measured in compliance with the methods and procedures described in the International Standard ISO 13660, related well to machine readability as measured according to the AIM International Technical Specification—Internal Symbology Specification Data Matrix.

Furthermore, the absolute print growth is a fundamental measure of ink/media interaction that permits categorizing couples of ink and paper and blurriness as an inkjet printing system parameter that should not be neglected in the design of machine-readable systems. In this study, we found that the maximum value for measured print growth is 100µm (4 mils). If grade A or B symbols are required (D' 70), then the minimum acceptable module size X=508µm(20 mils). Under those conditions a calculated value (using a mathematical model under development) of the maximum acceptable blurriness for good readability is 100µm(4 mil), value slightly higher than the minimum value found in this study (86µm(3.4 mil)).

In conclusion, machine readability of 2D symbology requires the control of both ink/paper interaction (print growth) and inkjet printing system parameter (satelliting/blurriness). The module size has to be commensurate to the print quality attributes that affect machine readability.

Correlation of Print Quality with Ink/Paper Characteristics

From Table 7, we can see that the primary print quality attributes that are a strong function of printers/papers are print growth and, to a lesser extent, blurriness. Figures 9 to 11 show the dependence of contact angle, the ultrasonic attenuation wetting time tw, and the slope on print growth, respectively.

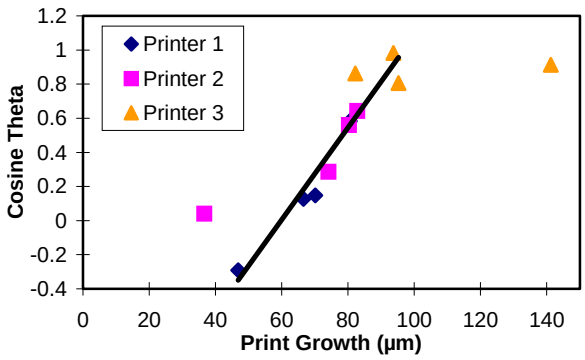

***Figure 9**. Relationship between contact angle and print growth*

We can see a definite trend: printer 3 ink with low contact angle produces the larger print growth on envelope I while printer 1 with a high contact angle (>90degrees) shows the lowest print growth, again on envelope I. For the rest of printers and papers there is a good correlation. The anomalies from the main correlation line are due to other paper charascteristics such as surface porosity, pH, and roughness.

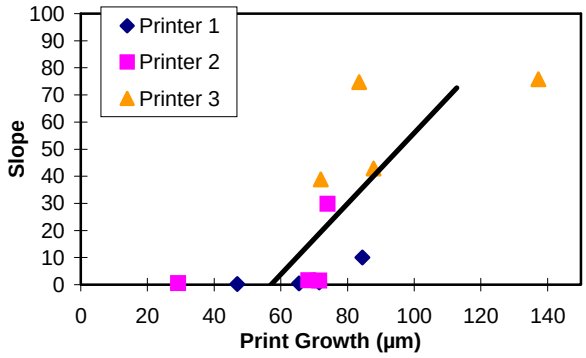

***Figure 10**. Relationship between ultrasonic attenuation slope and print growth*

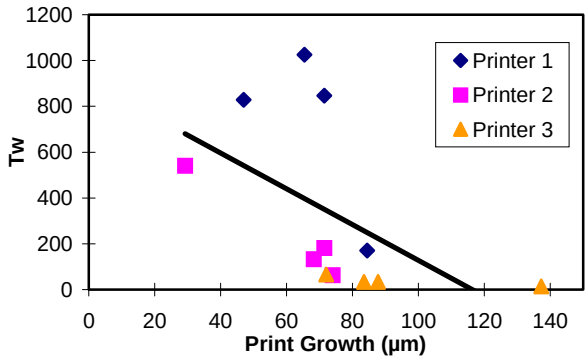

Figure 11. Relationship between Tw (wetting time) and print growth

Figures 10 and 11 show the dependence of print growth on the tw and slope from the ultrasonic attenuation data. Again, we can see a general tendency for print growth to increase with the slope (rate of penetration) that we would expect. The extremes are again envelope I with recycled fiber with printer 3 with a strongly wetting ink. Printers 1 and 2 with inks with high surface tension and high contact angle have a very low rate of penetration and consequently lower print growth. The graph of Tw (wetting time) shows a general trend of decrease of print growth with wetting time that, again, we would expect. The extremes are printers 2 and 1 with high contact angle inks and printer 3 with lower contact angle showing larger print growth.

Correlation between Ink/Paper Interactions and Print Quality Attributes

An examination of the results shows a general trend of increase in print growth (correlated well with raggedness as

seen in graph) with the decrease in contact angle. The measured contact angle is generally a result of the surface tension of the ink. Inks with lower surface tension wet better and generally have a lower contact angle. Therefore, we obtain extreme cases of print growth of 141µm for envelope I with ink H. Nevertheless, this ink shows a lower contact angle on the L envelope, but since the surface is more porous, the faster penetration prevents excessive bleeding and print growth is average and similar to the other samples. From the other side, the other two inks, C and F from printers 1 and 2, show a much lower print growth on envelope I (46 and 36µm as compared to the average of ~85µm). This effect again correlates well with the highest contact angle obtained on these substrates, and therefore the least amount of spreading. As we could see also from other references,[0] the spreading is enhanced by rough surfaces for liquids with contact angles less than ninety degrees and is inhibited by rough surfaces for contact angles greater than ninety degrees. Similar correlations are obtained with UA measurements. Again, for envelope I, ink H shows the shortest wetting time and largest slope, which correlates well with the large print growth values. For the same envelope I, the wetting times obtained are higher for inks C and F and exhibit low values for the rate of penetration (slope).

The Bristow curves that show the rates and profiles of liquid absorption into paper show the same extreme differences between the three inks on paper I: high rates of absorption of ink H (proportional to the square root of t according to classical Lucas Washburn behavior) as opposed to much lower rates (linear dependence on t) for inks C and F. The decrease of UEC with print growth shows that the tolerance of readability to a defined print growth is best for printer 2 and worst for printer 1. Printer 3, in spite of the largest print growth shown on envelope I (which is probably compensated by the lower blurriness), does not show the same fast rate of UEC decrease. We may note also, as a characteristic of diversity of substrates in these plots, that envelope I is shifting from the highest UEC tolerance to print growth (on the left side) for printers 1 and 2 to the lowest tolerance (on the right side) for printer 3. We may also remark that the values of print growth is high for the two envelopes containing recycled paper (I and L), which also contain the highest polar component in the critical surface energy values as shown in Table 2.

Conclusions

The requirements of the world's postal services to use 2D barcodes on envelopes is driving the need for better understanding of the relationships between print quality and 2D symbol readability. In inkjet printing, the strong dependance of print quality on ink/media interactions makes achieving consistently high print quality particularly challenging.

Measurements on a range of inkjet inks and envelope types show the strong dependance of print growth on ink contact angle and absorption rates. Smaller contact angles lead to increased print growth. This, in turn, leads to lower print quality and higher raggedness and blurriness, which lead to increased use of error correction bits and ultimately the failure to decode the 2D symbol. This paper develops a relationship between UEC and print growth and describes how it might be used statistically to predict read rates based on a given print quality.

Acknowledgements

The authors would like to thank Jay Reichelsheimer for his contributions to this paper by performing the printing and verifier tests as well as data plotting, and William Brosseau and Darel Gustafson for the print quality measurements and laser printer tests.

References

1. Information Based Indicia Program (IBIP), "Performance Criteria for Information Based Indicia and Security Architecture for Closed IBI Postage Metering Systems (PCIBI-C)," USPS, January 12, 1999
2. UPU Technical Standards Manual S28-1, "Communication of Postal Information using Two-Dimensional Symbols," 15 July 1998
3. Auslander J., Cordery R., and Zeller C., "Parameters Influencing Ink/Envelope Interaction and Bristow Absorption" *IS&T's NIP 13: International Conference on Digital Printing Technologies* 1997, pg. 450
4. Zeller C., Mackay D., Brosseau W., and Auslander J., *International Conference on Mail Technology- Tomorrow's World*, *IMechE*, published by Professional Engineering Publishing, Ltd. for the Institution of Mechanical Engineers, Bury St. Edmunds and London, UK, 1999, pg. 43
5. Auslander J., Zeller C., and Brosseau W., Information Based Indicia Program, *Technology Symposium Proceedings*, McLean, Virginia, November 25-26, 1996
6. Elftonson J. E. and Strom G., 1995 *Tappi Proceedings for Coating Fundamental Symposium*, pg 17
7. Lyne B. M., PRODUCTS OF PAPERMAKING, Transactions of the Tenth Fundamental Research Symposium held at Oxford: September 1993, published by Pira international, Vol. 2, pg 885
8. Bristow J. A., *Swensk Papperstids*, **70**, 623 (1967)
9. Owens, D. K. and Wendt, R. C., *Journal of Applied Polymer Science*, Vol. **13**, 1741 (1969)
10. Fox, H. V. and Zisman, W. A., Journal of Colloid and Fox, H. V., Zisman, W. A., *Journal of Colloid and Interface Sciences PTFE* , **5**: 514-531 (1950)
11. Bares, S. J., *Hewlett Packard Journal*, December 1988, pg 39
12. Pan Yun Long et al, *Tappi Journal*, Vol.**68**, No. 9. September 1985, pg 98
13. ISO/IEC 13660 "Measurement of image quality attributes for hardcopy output. Binary monochrome text and graphic images," 1997
14. ANSI/AIM BC11-1997, "International Symbology Specification—DataMatrix," Table N1, pg. 84

15. Zeller, C., Auslander, J., Brosseau, W., "Print Quality Parameters and Decodability of PDF 417 Two-Dimensional Symbology, Information Based Indicia Program," *Technology Symposium Proceedings*, McLean, Virginia, November 25-26, 1996
16. Brosseau, W, PB work in progress

Biography

Judith Auslander received her B.Sc. in Chemistry, M. Sc. in Organic Chemistry, and Ph. D. in Inorganic Chemistry, all from Hebrew University in Jerusalem. She joined Pitney Bowes in 1987 where she was responsible for developing inkjet inks for the piezo inkjet technology. She also developed fluorescent inks for franking and inkjet, new ink delivery systems based on ink-impregnated polymeric foams, and fluorescent thermal transfer ribbons used in Pitney Bowes's first digital postage meter. Most recently, she has studied the mechanism of ink/paper interactions between thermal transfer ribbons and commercial inkjet inks and various types of mailing envelopes. Dr. Auslander has 19 publications and holds 14 patents. She is a member of the IS&T and American Chemical Society.